Hind foot drumming: morphological adaptations of the muscles and bones of the hind limb in three African mole-rat species

L. Sahd[1], N.C. Bennett[2], S.H. Kotzé[1]

[1] Division of Clinical Anatomy, Department of Biomedical Sciences, Faculty of Medicine and Health Sciences, Stellenbosch University, Cape Town 8000, South Africa
[2] Department of Zoology and Entomology, Mammal Research Institute, University of Pretoria, Pretoria 0002, South Africa

Running Title: Hind limb morphology of African mole-rats
Editorial correspondence:
Prof S.H. Kotzé
Postal address: Department of Biomedical Sciences, Faculty of Medicine and Health Sciences, Stellenbosch University, PO Box 241, Cape Town, South Africa
Email: shk@sun.ac.za

ABSTRACT

Seismic signalling in the form of hind foot drumming plays an integral role in the communication of several species of African mole-rats (Bathyergidae). To produce these vibrational signals, alternating hind limbs strike the ground repetitively at high speeds by flexion and extension of the hip and knee. This descriptive study aimed to determine if anatomical differences in hind limb osteology and/or musculature between drumming and non-drumming species of three Bathyergidae species could be detected. Formalin fixed left and right hind limbs of 24 animals (N=48) consisting of three species (n=16 each) of two drumming species, *Georychus capensis* and *Bathyergus suillus*, and one non-drumming species, *Cryptomys hottentotus natalensis* were dissected in order to determine the origins and insertions of individual muscles. After dissection, all soft tissue was removed by maceration. Hind limb bones, including the pelvis, were photographed and the exact muscle origin and insertion points were electronically mapped onto the images using imaging software. On lateral view, the acetabular position was parallel to the sacrum in *G. capensis* while more ventral in position in the other two species. The shape of the femur head was spherical and the neck defined in all species. The distal shaft of the femur was gracile and the epicondyles robust and prominent in the non-drumming *C. h. natalensis* compared to the drumming species. Shallow and relatively wide patellar grooves were observed in all three species. In the two drumming species, *m. gracilis* was single while it was double in *C. h. natalensis*. In all three species, *m. tensor fasciae latae* was absent. The more dorsal positioning of the acetabulum in *G. capensis* may be needed to increase the stability of the spine and allow for more force to be exerted onto the pelvis during drumming. It is unlikely that *m. gracilis* plays a role in drumming as the singularity or doubling thereof is variable among rodents. It is additionally postulated that *m. gluteus superficialis* has taken the hip rotator role of *m. tensor fasciae latae* as it partially inserted onto the lateral fascia of the thigh. The more robust ilia, femoral shafts and tibiae observed in the two drumming species studied here are possible adaptations for hind foot drumming as robust bones are able to withstand the additional biomechanical loading during drumming.

KEY WORDS:

INTRODUCTION

Seismic signalling is a means of communication whereby information is conveyed to individuals of both conspecific and heterospecific species. These signals are generated via vibrations created by either the striking or drumming of part of the body on the ground or in some cases, low frequency vocalisations (Bennett & Jarvis, 1988; Hill, 2009; Randall, 2001; 2010). Hind foot drumming is the most common form of seismic signalling (Randall, 2001) and plays a vital ecological role in various rodent species including African mole-rats of the family Bathyergidae (Bennet & Faulkes, 2000). Drummers such as Bathyergidae generate foot drumming by striking the ground repeatedly and at high speed with alternating hind legs, moving the whole hind limb by flexion and extension of the hip and knee (Bennett & Jarvis 1988; Narins *et al.*, 1992). The speed and frequency of the seismic signals produced by hind foot drumming differ depending on the species and individual (Randall, 2010).

African mole-rats are fossorial rodents and the three species studied here namely, *Georychus capensis* (the Cape mole-rat; Pallas, 1778), *Bathyergus suillus* (the Cape dune-mole-rat; Schreber, 1782) and *Cryptomys hottentotus natalensis* (the Natal mole-rat; Roberts, 1913) are endemic to South Africa (Hart *et al.,* 2006; Bennett *et al.,* 2006; Bennett *et al.,* 2009).

Georychus capensis is a solitary mole rat and is reported to be aggressive and xenophobic. They engage in foot drumming to alert others to its presence and prevent interaction (Sherman *et al.*, 1991). Males initiate courtship with foot drumming; the actual mating is short, consisting of several sessions with foot drumming between sessions (Bennett & Faulkes, 2000; Bennett *et al.*, 2006). Males and females drum at different frequencies and speeds, with males drumming for two minutes at a rate of 26 beats (drums) per second, while females drum at a slower rate of 15 beats per second (Bennett & Jarvis 1988; Narins *et al.*, 1992; van Sandwyk & Bennett, 2005).

Bathyergus suillus is solitary, known to be highly territorial and aggressive towards others and engages in hind limb drumming to alert others of its presence and scare away rivals (Hart *et al.,* 2006). This species additionally uses seismic signals to advertise their readiness to mate. Their courtship behaviour includes a two-week period where males and females drum messages to each other with increasing frequency and speed, to the point where the males drum very fast (Sherman *et al.*, 1991; Hart *et al.*, 2006). Foot drumming has not been

reported in *C. h. natalensis* however, in some *Cryptomys hottentotus,* subspecies, occasional singular foot thumping has been reported (Lacey *et al.*, 2000).

The hind limb morphology of fossorial rodents has been rarely studied with preference given to the forelimb in order to study digging adaptations. However, hind limb musculature of mole-rats received some attention during the 19th and 20th Centuries, albeit somewhat fragmented. Dobson (1884) briefly discussed the anatomy of only two digital muscles (*m. flexor hallucis longus* and *m. flexor digitorum longus*) in *Bathyergus maritimus* (old classification of *B. suillus*). Hilderbrand (1978) reported the origin and insertions of three leg flexor muscles and the bones of the tarsus in an overarching study of 58 genera of rodents that included *Georychus, Bathyergus* and *Cryptomys* species. The latter study did not indicate the exact species or number of specimens that were examined. A more comprehensive study by Parsons (1896) described the whole body myology of an unspecified number of *G. capensis* and *B. maritimus* samples including the hind limb muscles. However, the study lacked detailed information on the osteology and the exact origins and insertions of the muscles. More recently, Özkan (2002) studied the osteology of the hind limb of another mole-rat species, *Spalax leucodon* (Lesser mole-rat), of the Spalacidae family of rodents.

Studies on whether the hind limb is morphologically adapted to allow high frequency foot drumming in mole rats are lacking. The present study therefore aims to provide a description of the osteology of the hind limb, including the pelvis, focusing on potential differences between two known drumming African mole-rat species (*G. capensis* and *B. suillius*) and one non-drumming species (*C. h. natalensis*). Furthermore, by studying the myology of the hind limbs, the study aims to detail and compare possible differences in the origins and insertions of the muscles of drumming and non-drumming species.

MATERIALS AND METHODS

Both left and right limbs of 24 animals (N=48 limbs), consisting of three species (n=16 each), were obtained from previous unrelated studies (Table 1). These species included *G. capensis* (the Cape mole-rat), *B. suillus* (the Cape-dune mole-rat) and *C. h. natalensis* (the Natal mole-rat). Ethical approval to work on the specimens was obtained from the Stellenbosch University Research Ethics Committee: Animal Care and Use (REC: ACU) with ethical clearance number SU-ACUM 16-00005.

Table 1 Species information including ethical approval, capture information and mean body mass. (± Standard deviation)

Species	Ethical approval	n	Capture site	Mean body mass (g)
Georychus capensis	University of Johannesburg: 215086650-10/09/15	8	Darling, Western Cape	213.89 ± 60.82
Bathyergus suillus	University of Cape Town: 200/V7/JOR	8	ACSA Cape Town, Western Cape	922.25 ± 233.47
Cryptomys hottentotus natalensis	University of Pretoria: ECO0070-14	8	Glengarry, Kwa-Zulu Natal	118.96 ± 30.63

The hind limbs of each specimen were dissected to the level of the origin and insertion sites of each muscle. The muscles, along with their exact origins, insertions and innervation were noted, after which all remaining soft tissue was removed using a maceration technique similar to that described by Bartels and Meyer (1991). Briefly, the specimens were placed into a 10% soap water solution made with automatic washing powder (*Bio Classic, Johannesburg, South Africa*). The specimens were heated to and maintained at 55°C using a slow cooker (*Sunbeam, Boca Raton, Florida, United States of America*) until the remaining soft tissue was easily removable. All bones were cleaned using a forceps and a scrubbing brush before study. High magnification images of the bones were taken using a Leica MZ6 stereomicroscope (*Leica microsystems, Oberkochen,* Germany). Subsequently, composite images were generated using AutoStitch v2.2 (demo version 2014). The origin and insertion sites of the muscles were mapped onto images of each species using GNU Image Manipulation Program (GIMP) imaging software.

RESULTS

Osteology

Pelvis

The pelvic bone of all three species (Figure 1 A to I) was similar and relatively straight with flat iliac wings (alae)*.* However, several differences were found between species: The body of the ilium was more gracile in *C. h. natalensis* compared to the two drumming species. On lateral view, in *G. capensis* the position of the acetabulum was almost parallel to the sacrum (Figure 1 A), while in *B. suillius* and *C. h. natalensis,* the acetabulum was situated ventral to
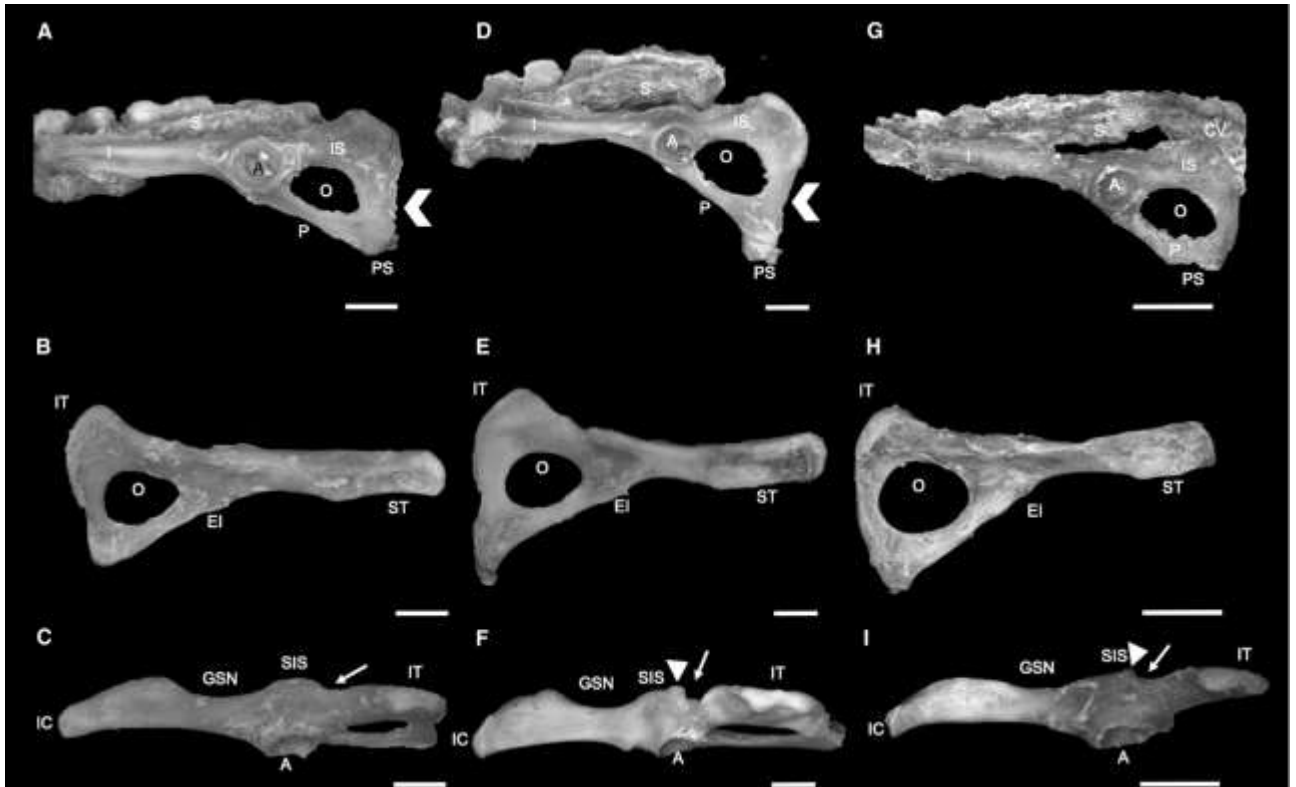
Figure 1. Left os coxae of three species of mole-rats seen in lateral (top, vertebral column and sacrum attached) medial (middle) and dorsal view (bottom), the two drumming species, *Georychus capensis* (A-C), *Bathyergus suillius* (D-F) and the non-drumming specie, *Cryptomys hottentotus natalensis* (G-I). The ilium was more gracile and the sacral tuberosity was small in *Cryptomys hottentotus natalensis* (G, H) compared to the two drumming species. In *G. capensis* the acetabulum was almost parallel to the sacrum (A), in *B. suillius* the acetabulum was more centrally located (D) and in *Cryptomys hottentotus natalensis* the acetabulum was situated the most ventral relative to the sacrum (G). The greater sciatic notch was more pronounced in *Georychus capensis* (C) and *Bathyergus suillius* (F) compared to *Cryptomys hottentotus natalensis* (I). The obturator foramen of *Cryptomys hottentotus natalensis* (G, H) was round compared to the more ovoid obturator foramen in the drumming species (A, B, D, E). The ischium and pubis were more demarcated by an indentation in the drumming species (white chevron; A, C) than in *Cryptomys hottentotus natalensis.* Acetabulum (A); Caudal vertebrae (CV); Illiopubic eminence (EI); Greater sciatic notch (GSN); Ilium (I); Iliac crest (IC); Ischium (IS); Ischial spine (SIS); Ischial tuberosity (IT); Lesser sciatic notch (white arrow); Obturator foramen (O); Pubic symphysis (PS); Sacrum (S); Sacral tuberosity (ST). White arrow head for tubercle on the ischial spine. Bar = 5 mm.

the level of the sacrum (Figure 1 D & G). The greater sciatic notch was more pronounced in the two drumming species and was deeper than the lesser sciatic notch (Figure 1 C, F & I). The lesser sciatic notch was the deepest in *B. suillius.* Furthermore, the ischiadic spine in *B. suillius* and *C. h. natalensis* had an extra tubercle each (Figure 1 C, F & I, white arrow head). The obturator foramen in *C. h. natalensis* was more round and relatively larger than that of the drumming species where the foramen was oval in shape (Figure 1 A, D &G). The body of the ischium was robust in the drumming species compared to being more gracile in *C. h. natalensis* (Figure 1 B, E & H). The ischial tuberosities were prominent in all three species. The junction between the ischiadic ramus and cranial pubic ramus of *C. h. natalensis* was continuous and had a rounded appearance compared to the indentation observed between the ischium and pubis in the two drumming species (Figure 1 A & D, white chevron).

Femur

Cranial, caudal and inferior views of the femurs are illustrated in Figure 2 (A to I). The head of the femur was spherical and the femoral neck well defined in all three species. The fovea capitis was pronounced in *B. suillius,* less distinct in *C. h. natalensis* and barely visible in *G. capensis* (Figure 2 A, C & E). Prominent greater, lesser and third trochanters were observed in all three species. In addition, the third trochanter extended caudally from the greater trochanter to a third of the length of the femur in all three species. The trochanteric fossa was relatively deep and bordered by a prominent intertrochanteric crest caudally in *B. suillius* (Figure 2 D) which was not pronounced in the other two species.

In *C. h. natalensis,* the distal femoral shaft was narrower and the femoral epicondyles more robust compared to the other two species (Figure 2 E). All three species had prominent and protuberant condyles and a deep intercondylar fossa. The patellar groove of the femoral trochlea was relatively shallow in all three species. However, the width of the patellar groove was the broadest in *C. h. natalensis* when compared to the other species (Figure 2 G, H & I). No sesamoid bones of the gastrocnemius muscle were observed in any of the species.

Patella

Cranial and caudal views of the patella are illustrated in Figure 3 (A to F). The patellae of *G. capensis* and *B. suillius* were roughly triangular with a rounded patellar apex (Figure 3 A & C). In contrast, the patella of *C. h. natalensis* was ovoid with a sharp patellar apex (Figure 3

Figure 2. The cranial (top), caudal (middle) and distal (bottom) aspects of the left femur of *Georychus capensis* (A-C), *Bathyergus suillus* (D-F) and *Cryptomys hottentotus natalensis* (G-I). The fovea capitis was pronounced in *Bathyergus suillius* (C), less distinct in *Cryptomys hottentotus natalensis* (G) and barely visible in *G.* capensis (A). The femoral neck was long and slender in *Georychus capensis* (A, B) and short and robust in *Cryptomys hottentotus natalensis* (E, F). The distal shaft of the femur was narrow in *Cryptomys hottentotus natalensis* and the epicondyle more pronounced (E, F) compared to the two drumming species. The patellar groove was shallow in all three species but broadest in *Cryptomys hottentotus natalensis* (G) Greater trochanter (GT); Head of femur (H); Intercondylar fossa (ICF); Lateral condyle (LC), Lateral epicondyle (LE), Lesser trochanter (LT), Medial condyle (MC); Medial epicondyle (ME); Patellar groove (PG); Shaft of the femur (S); Trochanteric fossa (TF); Third trochanter (TT); Intertrochanteric crest (black arrow); Bar = 5 mm (A, B, D, E, F, G, H). Bar = 3 mm in C and 2 mm in I.

E). The lateral articular surface of the patella was large in all three species and demarcated from the small medial articulation surface by a prominent vertical ridge.
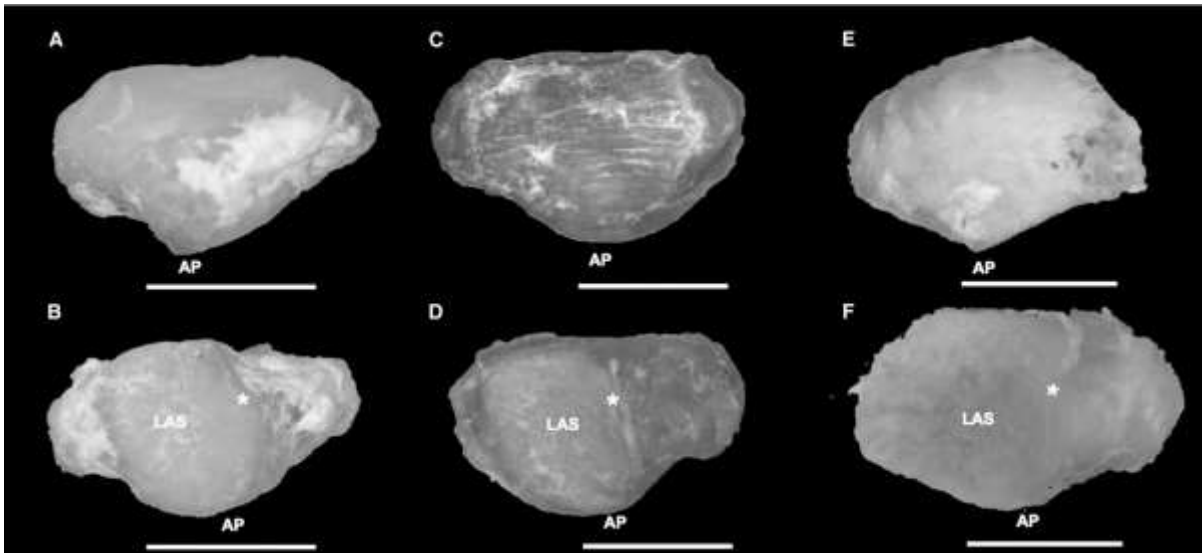

Figure 3. The cranial (top) and caudal (bottom) aspects of the patella of *Georychus capensis* (A & B; Bar = 3 mm), *Bathyergus suillius* (C & D; Bar= 5 mm) and *Cryptomys hottentotus natalensis* (E & F; Bar = 2 mm). The patellae of the two drumming species (*Georychus capensis* and *Bathyergus suillius*) were roughly triangular with a rounded apex (A, C) while the patella of *Cryptomys hottentotus natalensis* was ovoid with a sharp apex. Apex (AP); Lateral articular surface (LAS); * indicates the vertical ridge.

Tibia and Fibula

Lateral and medial views of the tibia and fibula are illustrated in Figure 4 (A to F). In all three species, a caudally directed fibular articular projection of the tibia was observed (Figure 4 A, C & E). The tibia of *C. h. natalensis* was more slender than in the two drumming species with a narrowing just ventral to the head of the tibia. In contrast, the tibial shaft in the drumming species, *B. suillus* and *G. capensis*, had no narrowing and was robust. The tibial tuberosity was prominent in all three species. The distal third of the tibia and fibula were fused in all three species (Figure 4). The fibula of all three species was gracile however, in *C. h. natalensis* the proximal fibula was angled medially and distinctly curved (Figure 4 E).

Tarsals and metatarsals, phalanges

The configuration of the tarsal bones (Figure 5) was similar in all three species. The proximal row of tarsal bones consisted of the calcaneus, talus and medial tarsal bone. The middle row consisted of the central tarsal bone which was connected to the talus and cuneiform bones. The distal row of tarsal bones was made up of the cuboid and three cuneiform bones. Two sesamoid bones were observed in all three species namely one in the tendon of insertion of *m. extensor digitorum longus* which articulated with the first cuneiform bone and
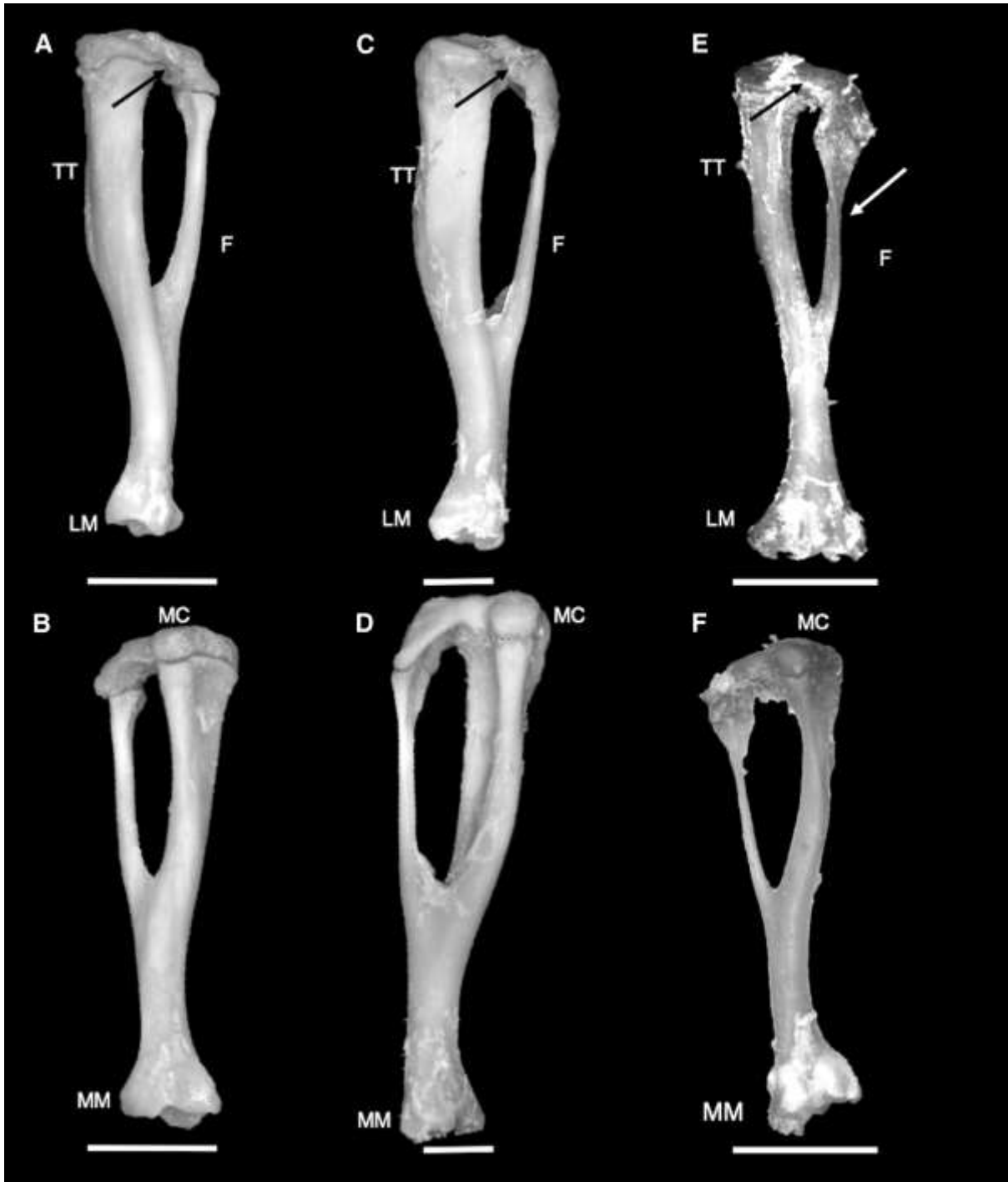
Figure 4. The craniolateral (top) and caudomedial (bottom) aspects of the tibia and fibula of *Georychus capensis* (A & B), *Bathyergus suillius* (C & D) and *Cryptomys hottentotus natalensis* (E & F). The tibias of the two drumming species (A, C) were more robust compared to *Cryptomys hottentotus natalensis*. The fibula of *Cryptomys hottentotus natalensis* (E) was medially curved as indicated by the white arrow. Fibula (F); Lateral malleolus (LM); Medial condyle (MC); Medial malleolus (MM); Tibial tuberosity (TT); Fibular articular projection (black arrow). Bar = 5 mm. Images of relatively young animals as growth plates are clearly visible.

the medial tarsal bone. A second sesamoid bone was found in the tendon of insertion of *m. peroneus digiti quinti* that articulated with the fifth metatarsal bone. All three species had five metatarsal bones with metatarsal III being the longest. In order of longest to shortest the metatarsals were arranged as follows MtIII> MtIV> MtII> MtV> MtI. All three species had five digits with three phalanges in digits two to five and two in digit one.
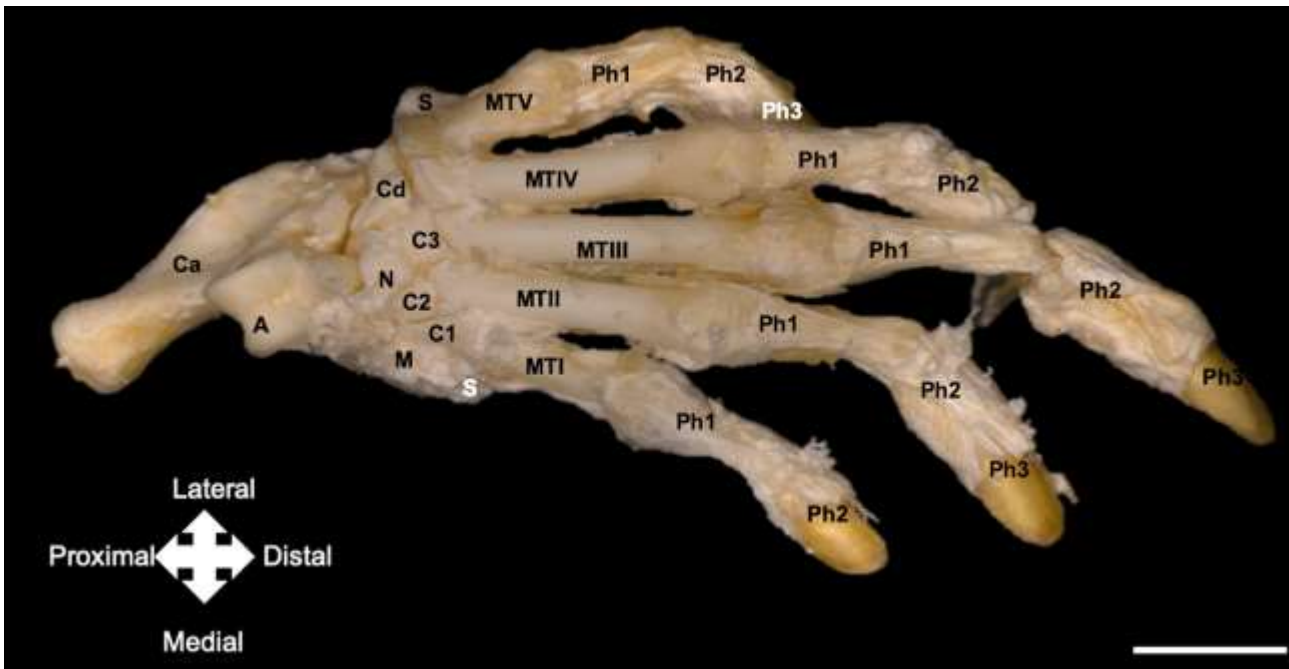

Figure 5. The dorsal view of the left pes of *Bathyergus suillius* as a representative of all three species, Bar = 5 mm. Astragalus (A); Calcaneus (Ca); Cuboid (Cd); Cuneiform (C1-3); Medial tarsal (M); Metatarsal (MT1-5); Navicular (N); Phalanx (Ph1-3); Sesamoid bone (S).

Muscle origins and insertions

The hind limb muscular arrangement, including origin and insertion sites, as well as innervation were similar in all three species (Figures 6 to 9 and Tables 2 to 4). However, the following difference was noted between species: the *m. gracilis* was a single muscle in the two drumming species (*G. capensis* and *B. suillius*) while cranial and caudal parts were present in the non-drumming *C. h. natalensis* (Figure 10). Differences between the animals in the present study and other rodents, included the absence of *m. tensor fasciae latae* in all three species (Figure 11). This was confirmed by the absence of a branch from the cranial gluteal nerve to the superficial gluteal muscle, which would have indicated fusion of *m. tensor fasciae latae* and *m. gluteus superficialis*. The muscle innervation of all three species did not differ from each other and was similar to that previously reported in the rat (Parsons, 1896; Greene, 1935).
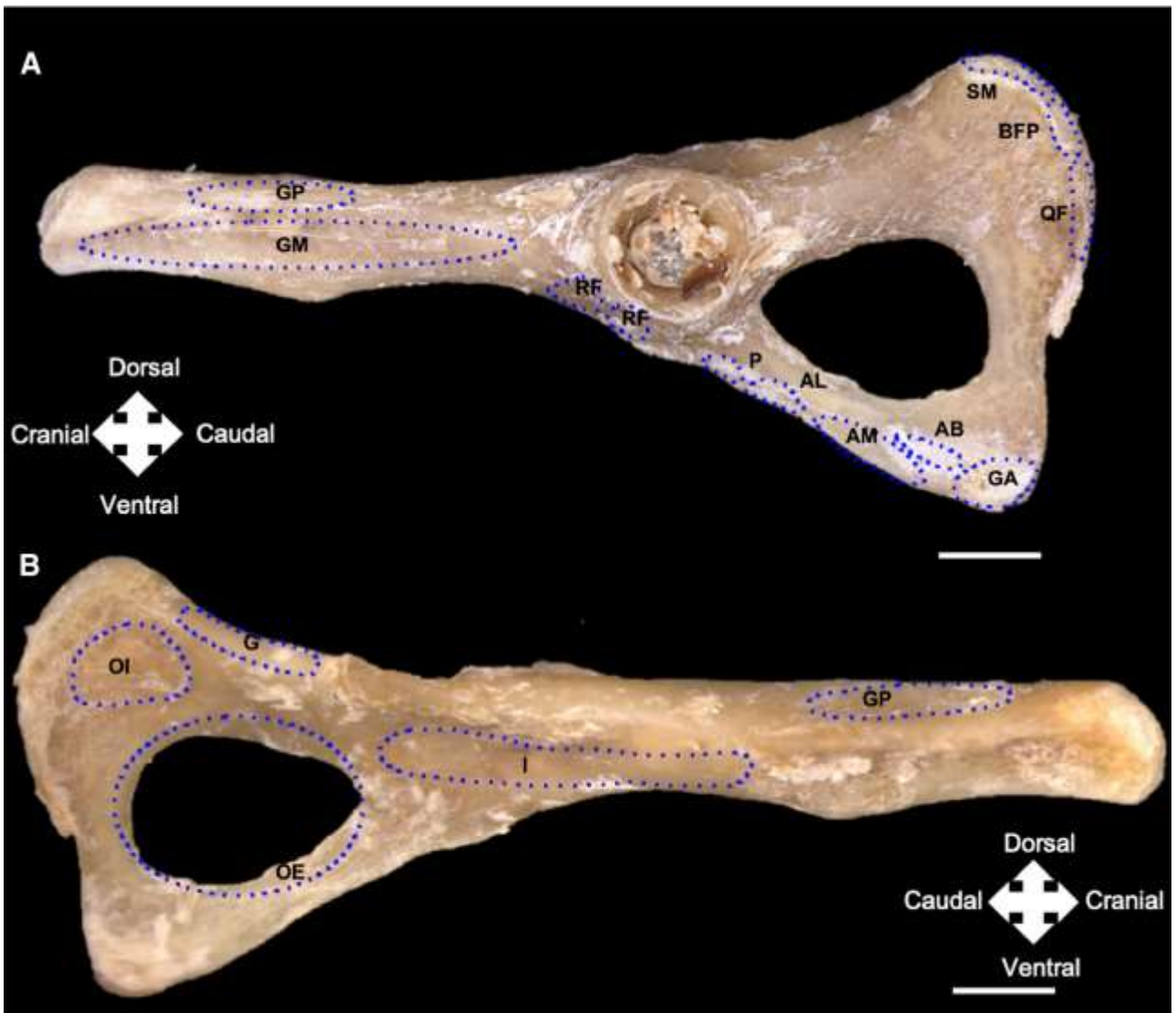
Figure 6. The origin (blue) sites of the muscles on the pelvis of *Georychus capensis* as representative of all three species. A. The lateral view of the pelvis. B. The medial view of the pelvis. *M. adductor brevis* (AB); *M. adductor longus* (AL); M. a*dductor magnus* (AM); M. b*iceps femoris* caudal head (BFP); *Mm. gemelli* (G); *M. gracilis anticus* (GA); *M. gluteus medius* (GM); *M. gluteus profundus* (GP): *M. illiacus* (I); *M. obturator externus* (OE); *M. obturator internus* (OI); *M. pectineus* (P); *M. quadratus femoris* (QF); *M. rectus femoris* (RF); *M. semimembranosus* (SM). Bar = 5 mm.
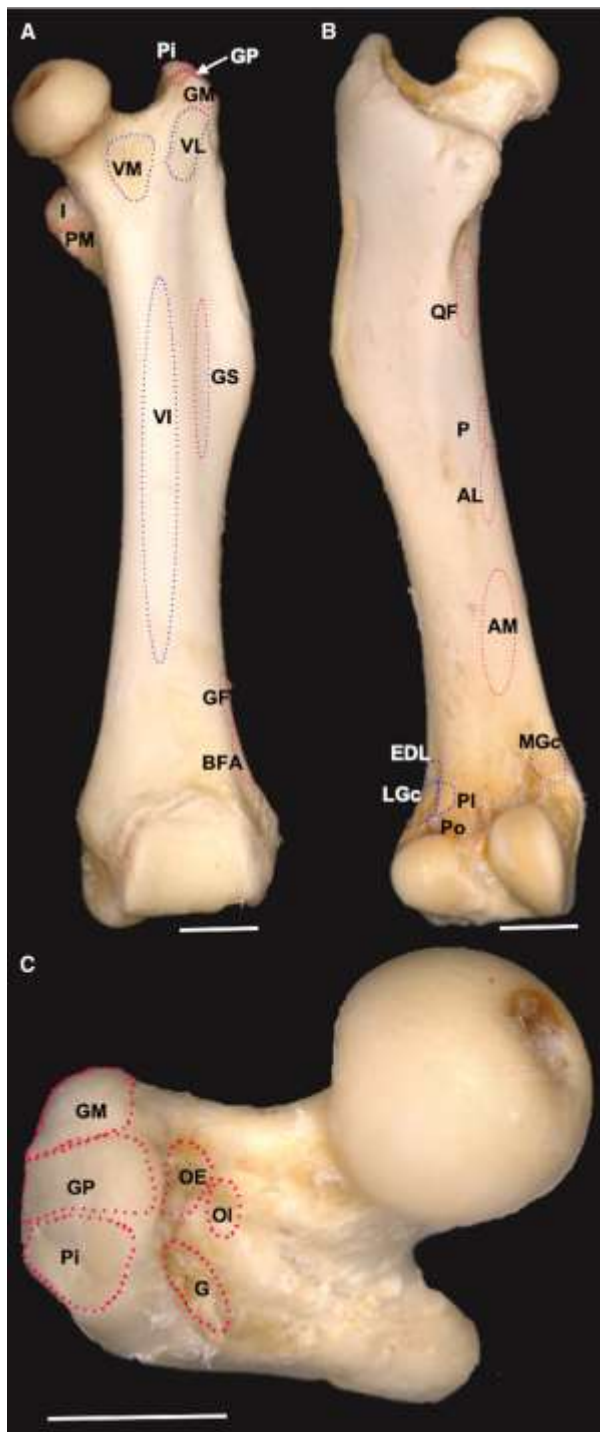
Figure 7. The origin (blue) and insertion (red) sites of the muscles on the femur of *Bathyergus suillius* as representative of all three species. A. Cranial view. B. Caudal view. C. Dorsal view. *M. adductor longus* (AL); *M. adductor magnus* (AM); *M. biceps femoris* cranial head (BFA); *M. extensor digitorum longus* (EDL); *M. gemelli* superior and inferior (G); *M. gluteofemoralis* (GF), *M. gluteus medius* (GM), *M. gluteus profundus* (GP); *M. gluteus superficialis* (GS); *M. illiacus* (I); Lateral head of *M. gastrocnemius* (LGc); Medial head of *M. gastrocnemius* (MGc); *M. obturator externus* (OE); *M. obturator internus* (OI); *M. pectineus* (P); *M. piriformis* (Pi); *M. plantaris* (Pl); *M. psoas major* (PM); *M. quadratus femoris* (QF); *M. vastus intermedius* (VI); *M. vastus lateralis* (VL); *M. vastus medialis* (VM). Bar = 5 mm.

Figure 8. The origin (blue) and insertion (red) sites of the muscles on the tibia and fibula of *Cryptomys hottentotus natalensis* as a representative of all three species. A. Cranial view. B. The Caudo-medial view. C. Cranio-lateral view. *M. extensor hallucis longus* (EHL); *M. flexor digitorum longus* (FDL); *M. flexor hallucis longus* (FHL); *M. gracilis anticus* (GA); M. g*racilis posticus* (GP); *Ligamentum patellae* (LP); *M. p*eroneus brevis (PB); *M. peroneus longus* (PL); *M. peroneus digiti quarti* (PD4); *M.peroneus digiti quinti* (PD5); *M. semimembranosus* (SM); *M. soleus* (S); *M. tibialis cranialis* (TA); *M. tibialis caudalis* (TP); *M. semitendinosus* (ST). Bar = 2.5 mm.
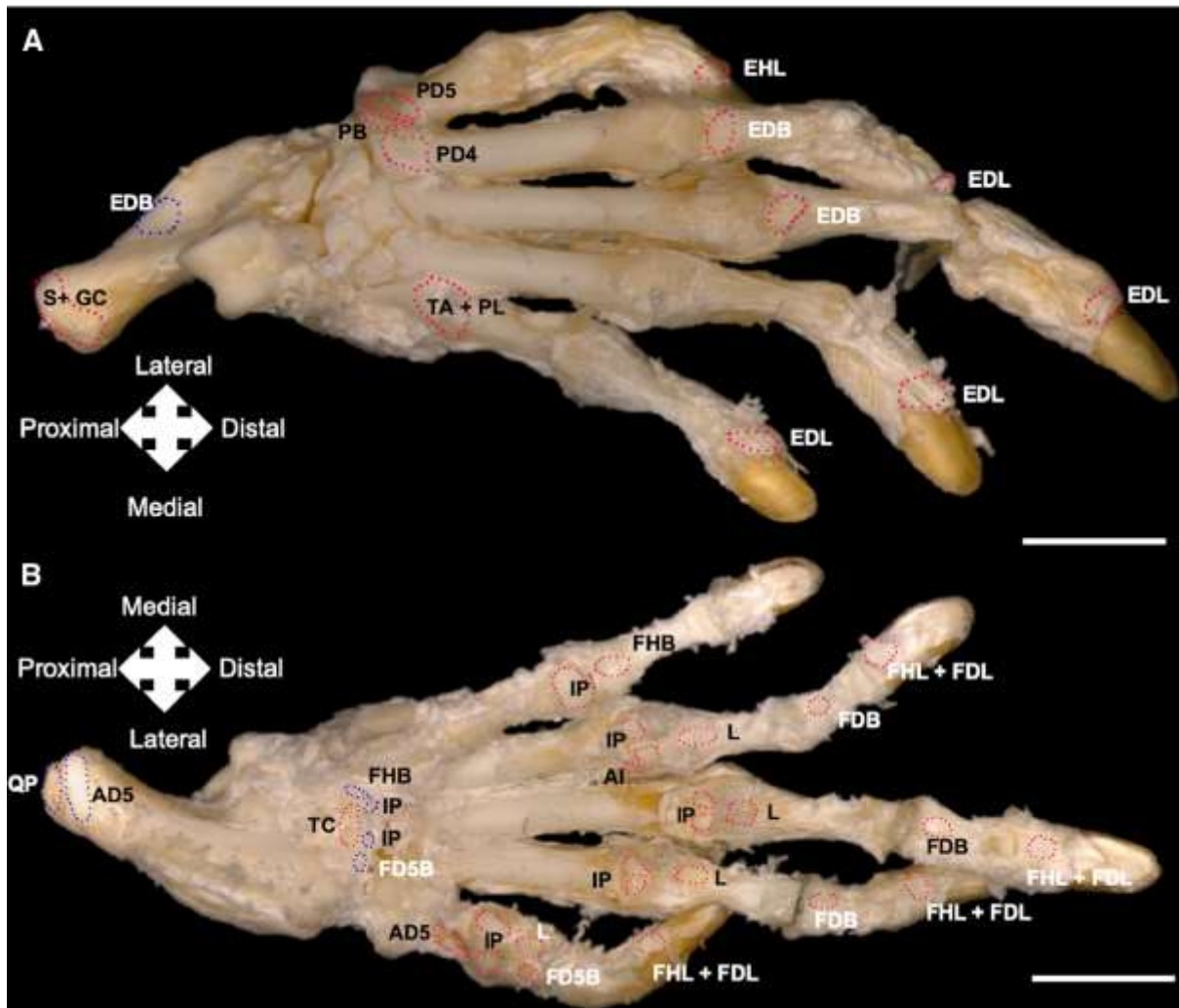
Figure 9. The origin (blue) and insertion (red) sites of the muscles on the left hind foot of *Bathyergus suillius* as representative of all three species. A. Dorsal view. B. Plantar view. *M. adductor indicis* (AI); *M. abductor digiti quinti* (AD5); *M. extensor digitorum brevis* (EDB); *M. extensor digiti longus* (EDL) *M. extensor hallucis longus* (EHL); *M. gastrocnemius* (GC); *M. flexor digitorum longus* (FDL); *M. flexor hallucis longus* (FHL); *M. flexor hallucis brevis* (FHB); *M. flexor digiti quinti brevis* (FD5B); *M. interossei plantaris* (IP); *Mm. lumbricales* (L); *M. p*eroneus brevis (PB); *M. peroneus longus* (PL); *M. peroneus digiti quarti* (PD4); *M. peroneus digiti quinti* (PD5); *M. quadratus plantae* (QP); *M. tibialis cranialis* (TA); *M. tibialis caudalis* (TP);. Bar = 5 mm.

Table 2. The origin, insertion, function and innervation of the muscles acting on the hip

Muscle	Functional Group	Origin	Insertion	Innervation
Gluteus superficialis	Hip extensors	Thoracolumbar fascia	Near the third trochanter	Caudal gluteal nerve & caudal branch of cranial gluteal nerve
Gluteus medius	Hip extensors	Ala of the lateral ilium	Greater trochanter of femur	Cranial gluteal nerve
Semitendinosus	Hip extensors knee flexors	Sacral and caudal vertebrae	Medial side of the tibial shaft caudal to *m. gracilis anticus*	Tibial division of sciatic nerve & a small branch form lumbro-sacral plexus
Biceps femoris (cranial)	Hip extensors knee flexors	Cranial facets of sacral and caudal vertebrae	Lateral side of the distal femur	Caudal gluteal nerve
Biceps femoris (caudal)	Hip extensors knee flexors	Tuber ischii	Crural fascia	Tibial division of sciatic nerve
Semimembranosus	Hip extensors knee flexors	Caudal edge of ischium	Medial surface of the proximal tibia cranial to *m. gracilis*	Tibial division of sciatic nerve
Gluteofemoralis	Hip extensors	Sacrum & 1st caudal vertebrae	Lateral side of the distal femur	Tibial division of sciatic nerve
Gluteus profundus	Hip rotators	Dorsal border of ilium	Greater trochanter of femur	Cranial gluteal nerve
Piriformis	Hip rotators	The lateral surface the spinous processes of the sacrum	Greater trochanter of femur	Branch of lumbro-sacral plexus (same as *Obturator internus*)
Quadratus femoris	Hip rotators	Posterior border of ischium caudal to *m. biceps femoris*	Medial side of the proximal femur close to the lesser trochanter	Posterior division of obturator nerve
Obturator internus	Hip rotators	Medial surface of ischium	Trochanteric fossa of femur	Nerve to the obturator internus from lumbro-sacral plexus
Gemelli superior & inferior	Hip rotators	Dorsal border of ischium	Trochanteric fossa of femur	Nerves form the lumbro-sacral plexus

Obturator externus	Hip adductors	Margin of obturator foramen	Trochanteric fossa of femur	Posterior division of obturator nerve
Tensor fascia latae	Hip rotators		Absent	
Adductor brevis	Hip adductors	Pubis caudal to *m. adductor magnus*	Tibial tuberosity via ligamentum patella	Posterior division of obturator nerve
Gracilus anticus	Hip adductors knee flexors	Pubic symphysis	Tibial shaft and aponeurotic insertion into the crural fascia	Anterior division of the obturator nerve
Gracilus posticus (only present in C. h. natalensis)	Hip adductors	Ramus of ischium	Tuberosity of tibia	Anterior division of the obturator nerve
Adductor longus	Hip adductor knee flexors	Ramus of pubis cranial to *m. adductor magnus*	Medial surface of the mid shaft of femur caudal to *m. pectineus*	Anterior division of the obturator nerve
Adductor magnus	Hip adductors	Pubis & pubic symphysis cranial to *m. adductor brevis*	Medial surface of the mid-distal shaft of the femur, caudal to *m. adductor longus*	Posterior division of obturator nerve
Iliacus	Hip flexors	Ventral iliac spine and iliac fossa of the ilium	Lesser trochanter of the femur	Second and third lumbar nerves
Psoas major	Hip flexors	Ventral surface of the bodies of the lower lumbar vertebrae	Lesser trochanter of the femur	Femoral nerve
Pectineus	Hip flexors	Pubic arch & iliopectineal tubercle	Media side of the proximal to mid shaft of femur cranial to *m. adductor longus*	Femoral nerve

Table 3. The origin, insertion and innervation of the muscles acting on the knee

Muscle	Functional Group	Origin	Insertion	Innervation
M. Quadriceps rectus femoris	Hip flexors knee extensors	Posterior head: Anterior border of acetabulum Anterior head: Ilium	Both heads insert on ligamentum patellae	Posterior division of the femoral nerve
M. Quadriceps vastus lateralis	Knee extensors	Greater trochanter of femur	Tuberosity of the tibia via ligamentum patella	Posterior division of the femoral nerve
M. Quadriceps vastus intermedius	Knee extensors	Cranial shaft of the femur	Tuberosity of the tibia via ligamentum patella	Posterior division of the femoral nerve
M. Quadriceps vastus medialis	Knee extensors	Neck and proximal end of femur	Tuberosity of the tibia via ligamentum patella	Posterior division of the femoral nerve
Gastrocnemius	Knee flexors Ankle plantarflexors	Medial & lateral epicondyles of femur	Tuber calcanei	Tibial nerve
Plantaris	Knee flexors Ankle plantarflexors	Lateral epicondyle of femur medial to the lateral head of *m. gastrocnemius*	Tendon of flexor digitorium brevis	Tibial nerve
Soleus	Ankle plantarflexors	Head of fibula caudal to *m. flexor hallucis longus*	Tuber calcanei	Tibial nerve
Popliteus	Knee flexors	Lateral epicondyle of femur caudal to *m. plantaris*	Medial side of the tibia distal to the medial condyle of the tibia	Tibial nerve

Table 4 The origin, insertion and innervation of the muscles acting of the ankle

Muscle	Functional Group	Origin	Insertion	Innervation
Tibialis cranialis	Ankle dorsiflexors	Lateral condyle, tuberosity and ventral crest of tibia	1st cuneiform & 1st metatarsal	Deep peroneal nerve
Extensor digitorum longus	Ankle dorsiflexors	Lateral epicondyle of femur cranial to the lateral head of *m. gastrocnemius*	3rd phalanx of digits 2-5	Deep peroneal nerve
Extensor hallucis longus	Ankle dorsiflexors	Distal ¼ of fibula	Last phalanx of hallux	Deep peroneal nerve
Flexor digitorum longus	Ankle dorsiflexors	Medial surface of the tibia cranial *to* *m. semimembranosus*	3rd phalanx of 2nd-5th digit with *m. flexor hallucis longus*	
Flexor hallucis longus	Ankle plantarflexors	Head of the fibula & the tip of the fibular projection of the tibia	3rd phalanx of 2nd-5th digit with *m. flexor digitorum longus*	Tibial nerve
Tibialis caudalis	Ankle plantarflexors	Proximal ends of tibia & fibula	Navicular 1st cuneiform	Tibial nerve
Peroneus longus	Ankle everters	Head of fibula	1st metatarsal & 1st cuneiform	Superficial peroneal nerve
Peroneus brevis	Ankle everters	The lateral surface of the midshaft of the fibula & interosseous membrane	5th metatarsal	Superficial peroneal nerve
Peroneus digiti quarti	Ankle everters	Head of fibula caudal to *m. peroneus longus*	4th metatarsal	Deep peroneal nerve
Peroneus digiti quinti	Ankle everters	Lateral shaft of fibula cranial to *m. peroneus brevis*	5th metatarsal	Deep peroneal nerve

Table 5: The origin and insertion of the muscles of the foot

| Muscle	Origin	Insertion	Innervation
Abductor digiti quinti	Calcaneus	5th metatarsal	Lateral plantar nerve
Quadratus plantae	Calcaneus	Tendons of *m. flexor digitorum longus* and *m. flexor hallucis longus*	Lateral plantar nerve
Lumbricles	Tendon of *m. flexor hallucis longus*	1st phalanx of digits 2-5	Lateral and medial plantar nerves
Flexor hallucis brevis	Navicular	1st phalanx of hallux	Medial plantar nerve
Flexor digiti quinti brevis	Cuboid	1st phalanx of digit 5	Lateral plantar nerve
Adductor indicis	Interosseous tendon of 3rd digit	Sesamoid of 2nd digit	Medial plantar nerve
Interossei plantaris	Navicular & cuboid	Metatarsals 1-5	Lateral plantar nerve
Flexor digitorum brevis	Tendon of *m. plantaris*	2nd phalanx of digits 2-4	Medial plantar nerve
Extensor digitorum brevis	Calcaneus	2nd phalanx of digits 2 & 3	Deep peroneal nerve
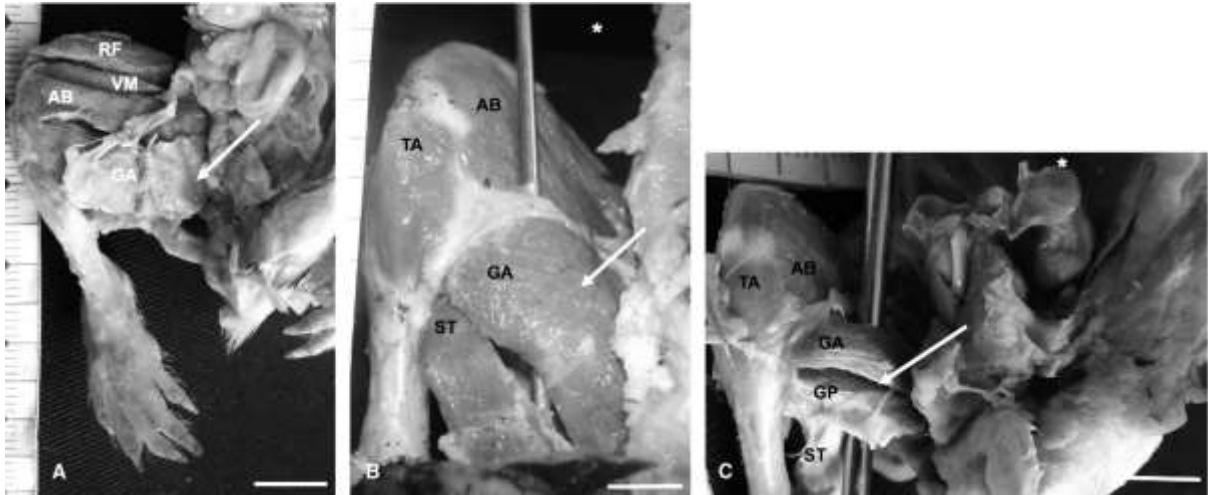
Figure 10. The medial view of the right hind limb of all three species showing the single *m. gracilis* in *Georychus capensis* (A) and *Bathyergus suillius* (B) and the double *m. gracilis* in *Cryptomys hottentotus natalensis* (C) as indicated by the white arrow. *M. adductor brevis* (AB); *M. gracilis anticus* (GA); *M. gracilis posticus* (GP); *M. rectus femoris* (RF); *M. semitendinosus* (ST); *M. tibialis cranialis* (TA); *M. vastus medialis* (VM). * indicates the direction of the head. Bar = 10 mm.
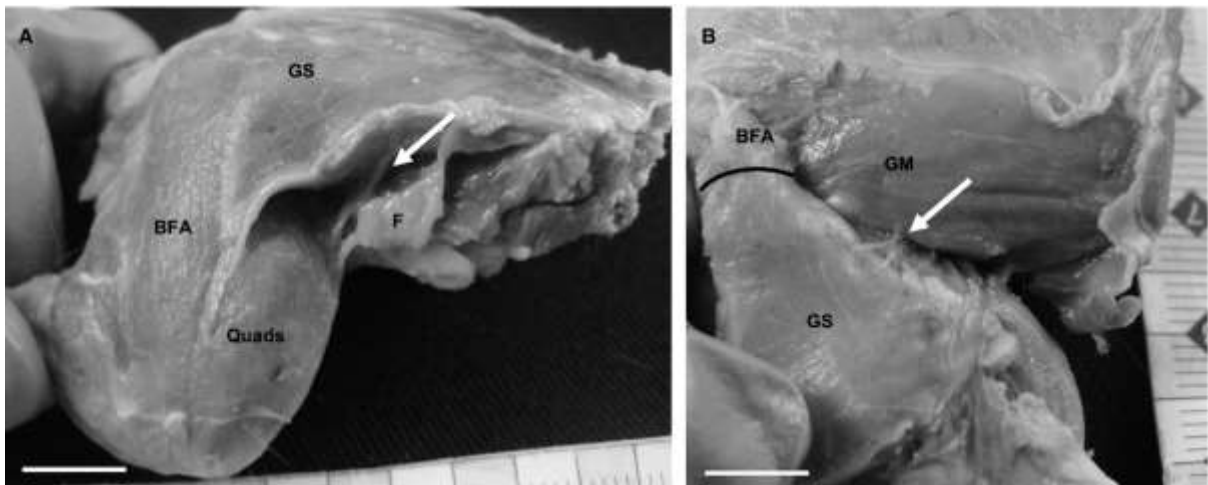

Figure 11. The lateral view of the right hind limb of *Georychus capensis* as a representative of all three species highlighting the absence of *M. tensor fasciae latae.* A. *M. gluteus superficialis* in original position. B. *M. gluteus superficialis* reflected. *M. biceps femoris* anterior head (BFA); Fat (F); *M. gluteus medius* (GM); *M. gluteus superficialis* (GS). Single innervation to GS by the superior and inferior gluteal nerves (white arrow). Black line demarcates *m. gluteus superficialis* and the anterior head of *m. biceps femoris*. Bar = 10 mm.

DISCUSSION

The pelvis of fossorial species such as mole-rats, moles and insectivores is orientated horizontally, parallel to the vertebral column. The position of the acetabulum in line with the sacrum is hypothesised to reduce the amount of torsion exerted on the spine during digging (Chapman, 1919). However, in the present study this arrangement was only found in *G. capensis* and not in the other two Bathyergidae species The ilium is the origin site of *m. gluteus medius,* one of the main hip extensors, and *m. iliacus*, one of the main hip flexors. The robust nature of the ilium and the position of the acetabulum parallel to the sacrum in *G. capensis* could allow for additional forces exerted on the pelvis during high speed hind foot drumming (Van Sandwyk & Bennett, 2005) and may be the reason why the pattern was not seen in the slower drumming *B. suillus.*

In the subterranean mole-rat *Spalax leucodon* (lesser mole-rat) of the Spalacidae family of rodents, the greater sciatic notch was more pronounced (Özkan, 2002) than observed in the Bathyergidae species studied here. The ischial spine of *G. capensis* was small with a rounded edge similar to that described in *S. leucodon* (Özkan, 2002). In contrast, the ischial spine of *B. suillius* and *C. h. natalensis* each had a small pointed tubercle. A large ovoid obturator foramen as observed in *G. capensis and B. suillius* is similar to that described in the non-drumming mole-rat *S. leucodon* (lesser mole-rat; Özkan, 2002). Additionally, ovoid obturator foramina are described in several non-drumming terrestrial rodent species including *Chinchilla langeria* (Chinchilla; Çevik-Demirkan *et al.,* 2007); *Cricetomy gambianus* (African giant rat; Olude *et al.,* 2009) and the semi-aquatic *Hydrochoerus hydrochaeris* (capybara; Brombini *et al.,* 2018). The round obturator foramen observed in *C. h. natalensis* is similar to that of terrestrial *Rattus norvegicus* (rat, Greene, 1935). It is therefore unlikely that the shape of the obturator foramen plays a functional role in either hind foot drumming or fossoriality.

Polly (2007) states that the four main features of the femur likely to be adapted for function are the shape of the femoral head, the length and orientation of the greater trochanter, the size of the third trochanter and the depth of the patellar groove on the femoral trochlea. The spherical head of the femur and defined femoral neck in the present study are consistent to that described in several non-fossorial and non-drumming rodent species (de Araujo *et al.,* 2013; Wilson & Geiger, 2015; Brombini *et al.,* 2018) and is therefore unlikely to have an influence on drumming. The greater, lesser and third trochanters are some of the main muscle attachment sites on the femur (Wilson & Geiger, 2015). The prominent greater and

lesser trochanters observed in the Bathyergidae species studied here were similar to that described in the non-drumming *S. leucodon* (lesser mole-rat; Özkan, 2002) and is likely to be a fossorial adaptation. In none of the species studied here, did the greater trochanters extended beyond the head of the femur like that observed in several semi-fossorial non-drumming *Typanoctomys* species (visacha rats; Perez *et al.,* 2017) and the non-fossorial *H. hydrochaeris* (capybara; de Araujo *et al.*, 2013). The size and position of the third trochanter are variable among rodent species (Wilson & Geiger, 2015) showing the following configurations. Firstly, the absence or under-developed third trochanter as seen in *C. langera* (Chinchilla; Çevik-Demikan *et al.*, 2007). Secondly, a small third trochanter situated in the distal third of the femur has been reported in the semi-aquatic *H. hydrochaeris* (capybara; de Araujo *et al.*, 2013; Garcia-Esponda & Candela, 2015; Brombini *et al.,* 2018), *Cunuculus paca* (paca; de Araujo *et al.,* 2013) and four semi-fossorial *Tympanoctomys* species (visacha rats; Perez et al., 2017). Lastly, a prominent well-developed third trochanter arising caudal to the greater trochanter and extending to the distal shaft of the femur as seen in all three mole-rats of the present study. The latter configuration was also seen in the terrestrial *Rattus norvegicus* (rat), *Cavia porcellus* (guinea pig; de Araujo, *et al.*, 2013) and a non-drumming mole-rat species *S. leucodon* (lesser mole-rat; Özkan, 2002). Therefore, the position and size of the trochanters of the femur are unlikely to play a role in hind foot drumming or fossoriality.

Deep patellar grooves on the femoral trochlea provide stabilisation for the knee through the patellar ligament (Polly, 2007; Wilson & Geiger, 2015). Whereas broad, shallow patellar grooves have been indicated to increase mobility in the knee joint, specifically flexion of the hind limb (White, 1993). In the present study, all three species had shallow patellar grooves indicating that the knee joint is highly mobile. This may be a fossorial adaptation allowing for increased mobility of the joint due to the fact that these species navigate confined spaces in their burrow systems.

The prominent femoral epicondyles of *C. h. natalensis* were emphasised by the narrow distal shaft of the femur compared to the robust nature of the femur in the two drumming species. The shaft of the femur is the insertion site for several hip extensors (the anterior head of *m. biceps femoris* and *m. gluteofemoralis*) and hip adductors including *m. pectineus* which acts as a stabilising force during flexion and extension of the hip as needed in drumming (Greene, 1935; Johnson *et al.,* 2008; Garcia-Esponda & Candela 2015). Furthermore, the tibias of the two drumming species were robust compared to *C. h. natalensis*. The medial surface of

the tibia is the insertion point for several knee flexors, knee extensors as well as the hip extensor, *m. adductor brevis*. Based on the premise of bone functional adaptation as explained by Ruff *et al.* (2006), the additional biomechanical load these muscles exert during hind foot drumming may have caused the more robust nature of the shafts of the femur and tibia.

The caudally directed fibular articular projection of the tibia observed in the Bathyergidae studied here has a similar shape to that of the terrestrial *C. paca* (paca; de Araujo, *et al.,* 2013) and four semi-fossorial *Tympancotomys* species (viscacha rats; Perez *et al.,* 2017). Furthermore, fibular articulation processes have been observed in several rodent species including the fossorial *S. leudcodon* (lesser mole-rat; Özkan, 2002) and non-fossorial Chinchilla species (Çevik-Demirkan, *et al.,* 2007). It is therefore unlikely that the fibular articular projection plays a role in either fossoriality or hind foot drumming as it is a common feature in various rodent species that exhibit a variety of locomotor behaviours.

Extensive fusion of the distal third of the tibia and fibula was observed in all species of the present study and is similar to that described in the fossorial *S. leucodon* (lesser mole-rat; Ozkan, 2002), but also seen in the terrestrial *R. norvegicus* (rat; Barnett & Napier, 1953; Moss, 1977) and *C. gambianus* (African giant rat; Olude *et al.*, 2009). Less extensive distal fusion of the tibia and fibula was reported in four *Tympancotomys* species (vischas rats; Perez *et al.,* 2017). According to Barnett & Napier (1953) fusion of the tibia and fibula may allow for sudden rapid movement of the hind limb. However, this has been observed in both drumming and non-drumming species studied here as well as fossorial and non-fossorial rodent species. Therefore it is unlikely that the fusion of the tibia and fibula plays a significant role in hind foot drumming or fossoriality.

The tarsal bones observed in the three species of the present study conforms to that described in several species of rodents including other non-drumming mole-rat species such as *S. leucodon* (Özkan, 2002) and an unspecified *Tachyoryctes* species (Hildebrand, 1978). Furthermore, the configuration of the tarsus in all three species conformed to that described in unspecified *Georychus, Bathyergus* and *Cryptomys* specimens studied by Hildebrand (1978). In the present study eight tarsal bones, five metatarsals and five digits were identified in all three species. The prominent medial sesamoid bone in the tendon *of m. extensor digitorum longus* attaching to the medial tarsal and first cuneiform bones observed in all three species was also noted by Hildebrand (1978).

The myology observed in the present study is similar to that described by a very early study of Parsons (1896) with the exception of *m. gracilis*. In the present study *G. capensis and B. suillius* both had a single *m. gracilis* and not two distinct cranial and caudal parts as described by Parsons (1896), while *C. h. natalensis* had both parts of the *m. gracilis*. The two distinct parts of *m. gracilis* seen in *C. h. natalensis* have been described in another fossorial rodent *Ctenomys talarum* (Talas tuco-tuco; Garcia-Esponda & Candela, 2015) but has also been seen in the non-fossorial *R. norvegicus* (rat; Greene, 1935) and *Mus musculus* (mouse; Charles *et al.*, 2016). However, the single m. gracilis of *G. capensis* and *B. suillius* followed a similar arrangement to that observed in non-fossorial rodents and moles (Gupta, 1966; McEvoy, 1982; Whidden, 2000; Garcia-Esponda & Candela, 2015). Therefore, the singularity or doubling of the *m. gracilis* is unlikely to have an effect on fossoriality or drumming using extension and flexion of the hip and knee. Klingener (1964) reported a single *m. gracilis* in a bipedal foot drumming rodent *Jaculus jaculus* (lesser Egyptian jerboa), but bipedal drummers utilise a different method of foot drumming, namely the flexion and extension of the ankle joint while balancing on their tail (Randall, 2014).

Parsons (1896) reported the absence of *m. tensor fasciae latae* in *G. capensis*, but the presence thereof in *B. martimus* (old classification of *B. suillius*). This is in contrast to the present study where the muscle was not observed in any of the species studied. Greene (1935) states that the *m. tensor fasciae latae* is often fused to *m. gluteus superficialis* in *Rattus norvegicus* (rat) and receives innervation from both the cranial and caudal gluteal nerves. However, in the present study, only one branch from the cranial gluteal nerve was present innervating only the caudal part of *m. gluteus superficialis* indicating that there was no fusion of the two muscles. Therefore, we postulate that the *m. gluteus superficialis* compensates for the absence of *m. tensor fasciae latae* by partially inserting onto the lateral fascia of the thigh, in order to additionally play a role as a hip rotator. Few differences in origins and insertions were noted between the drumming and non-drumming species studied here. Rabey *et al.,* (2015) suggested that locomotion and movement do not have an effect on the origin and insertion sites of muscles, but rather that the muscle architecture such as fibre type, physiological cross section area and volume are influenced more readily by movement adaptions.

Conclusion

The robust ilia, femoral shafts and tibiae observed in the two drumming species studied here are possible adaptations for hind foot drumming as more robust bones are able to withstand

the additional biomechanical loading exerted by extensors and flexors of the hip and knee joints during drumming.

ACKNOWLEDGEMENTS

AUTHOR CONTRIBUTIONS

Lauren Sahd performed the dissections, examined the bones, created the images and drafted the manuscript. Nigel Bennett provided the samples and edited the manuscript. Sanet Kotzé was the principle investigator, designed the project and edited the manuscript.

REFERENCES

Barnett, C.H. & Napier, J.R. 1953. The rotary mobility of the fibula in eutherian mammals. *Journal of Anatomy* 87: 11-21.

Bartels, T. H. & Meyer, W. 1991. Eine schnelle und effektive Methode zur Mazeration von Wirbeltieren. *Duetche Tierärztliche Wochenschrift* 98: 407- 409. Bennett, N.C. & Faulkes, C.G. 2000. *African mole-rats: Ecology and Eusociality.* Cambridge: Cambridge University Press. Taylor,

Bennett, N.C., Faulkes, C.G., Hart, L. & Jarvis, J.U.M. 2009. *Bathyergus suilus* (Rodentia: Bathyergidae). *Mammalian Species* 828: 1-7.

Bennett, N.C, & Jarvis, J.U.M. 1988. The reproductive biology of the Cape mole-rat, *Georychus capensis* (Rodentia: Bathyergidae). *Journal of Zoology, London.* 214:95-106.

Bennett, N.C., Maree, S. & Faulkes, C.G. 2006. *Georychus capensis. Mammalian Species* 799: 1-4.

Brombini, G.C., Rahal, S.C., Schimming, B.C., et al. 2018. Radiological and osteological study of the pelvic limbs in free-ranging capybaras (*Hydrochoerus hydrochaeris*). *Antomina Histologia Embryoloia* 47: 239-249.

Çevik-Demirkan, A., Özdemir, V., Türkmenoglu, I. & Demirkan, I. 2007. Anatomy of the hind limb skeleton of the chinchilla (*Chinchilla lanigera*). *Acta Veterinaria* 76: 501-507.

Chapman, R.N. 1919. A study of the correlation of the pelvic structure and the habits of certain burrowing mammals. *American Journal of Anatomy* 25: 184-219.

Charles, J. P., Cappellari, O., Spence, A.J., Hutchinson, J.R. & Wells, D.J. 2016. Musculoskeletal geometry, muscle architecture and functional specialisations of the mouse hindlimb. *PLos One* 11: e0147669. Doi:10.1371/journal.pone.0147669.

de Araujo, F.A.P., Sesko, N.F., Rahal, S.C., Texeira, C.R., Muller, T.R. & Machado, M.R.F. 2013. Bone morphology of the hind limbs in two caviomorph rodents. *Anatomia Histologia Embryologia* 42: 114-123.

Dobson, G.E. 1884. On the comparative variability of bones and muscles with remarks on unity of type of the origin and insertion certain muscles in species unconnected by unity of descent. *Journal of Anatomy* 19: 16-23.

Garcia-Esponda, C. & Candela, A.M. 2015. The hip adductor muscle group in caviomorph rodents: anatomy and homology. *Zoology* 118: 203-212

Greene, E. C. 1935. The anatomy of the rat. *Transactions of the American Philosophical Society* 27: 1-370.

Gupta, B.B. 1966. The anatomy of the posterior axial region and the hind limb of the Eastern American Mole. *Mammalia* 30: 667-682.

Hart, L., O'Riain, M.J., Jarvis, J.U.M. & Bennett, N.C. 2006. The pituitary potential for opportunistic breeding in the Cape dune mole-rat, *Bathyergus suillus. Physiology & Behaviour* 88: 615-619.

Hilderbrand, M. 1978. Insertions and functions of certain flexor muscles in the hind leg of rodents. *Journal of Morphology* 155: 111-122.

Hill, P.M. 2009. Vibration and Animal Communication: A Review. *American Zoologist* 41: 1135-1142.

Johnson, W.L., Jindrich, D.L., Roy, R.R.& Edgerton, V.R. 2008. A three-dimensional model of the rat hindlimb: Musculoskeletal geometry and muscle moment arms. *Journal of Biomechanics* 41: 610-619.

Klingener, D. 1964. The comparative myology of four dipoid rodents (genera *Zapus, Napaeozapus, Sicista* and *Jaculus*). *Miscellaneous Publications Museum of Zoology, University of Michigan* 124: 5-100.

Lacey, E.A., Patton, J.L. & Cameron, G.N. (eds). 2000 *Life underground; the biology of subterranean rodents.* Chicago: The University of Chicago Press.

McEvoy, J.S. 1982. Comparative myology of the pectoral and pelvic appendages of the North American porcupine (*Erethizon dorsatum*) and the prehensile-tailed porcupine (*Coendou prehensilis*). *Bulletin of the American Museum of Natural History* 173: 337-421.

Moss, M.L. 1977. A functional analysis of fusion of the tibia and fibula in the rat and mouse. *Acta Anatomica* 97: 321-332.

Narins, P.M., Reichman, O.J., Jarvis, J.U.M. & Lewis, E.R. 1992. Seismic signal transmission between burrows of the Cape mole-rat, *Georychus capensis. Journal of Comparative Physiology A* 170: 13-21.

Olude, M.A., Olopade, J.O. & Mustapha, O.A. 2009. Macro-anatomical investigations of the skeletons of the African giant rat (*Cricetomys gambianus* Waterhouse): Pelvic limb. *European Journal of Anatomy* 13: 127-131

Özkan, Z.E. 2002. Macro-anatomical investigations on the hind limb skeleton of mole-rat (*Spalax leucodon* Nordmann). *Veterinarski Arhiv* 72: 159-166.

Parsons, F.G. 1896. Myology of Rodents- Part II. An account of the myology of the Myomorpha, together with a comparison of the muscles of the various suborders of rodents. *Journal of Zoology* 64: 159-192.

Perez, M.J., Barquez, R.M. & Diaz, M.M. 2017. Morphology of the limbs in the semi-fossorial desert rodent species of *Tympanctomys* (Octodontdae, Rodentia). *ZooKeys* 710: 77-96.

Polly, P.D. 2007. Limbs in Mammalian Evolution, in in Hall, B.K. (ed). *Fins into Limbs: Evolution, Development and Transformation.* Chicago and London; Chicago University Press. 245-268.

Rabey, K.N., Green, D.J., Taylor, A.B., Begun, D.R., Richmond, B.G. & McFarlin, S.C. 2015. Locomotor activity influences muscle architecture and bone growth but not muscle attachment site morphology. *Journal of Human Evolution* 78: 91-102.

Randall, J.A. 2001. Evolution and function of drumming as communication in mammals. *American Zoologist* 41: 1143-1156.

Randall, J.A. 2010. Drummers and stompers: Vibrational communication in mammals, in C.E. O'Connell-Rodwell (ed). *The use of vibrations in communication: Properties, mechanisms and function across Taxa.* Kerala: Transworld Research Network: 100-120.

Randall, J.A. 2014. Vibrational communication: Spiders to Kangaroo rats. In: Wtzany, G. *Biocommunication of Animals.* 103-133.

Ruff, C., Holt, B. & Trinkhaus, E. 2006. Who's afraid of the big bad Wolff?: "Wolff's Law" and bone functional adaptation. *American Journal of Physical Anthropology* 129: 484-498.

Sherman, P.W., Jarvis, J.U.M. & Alexander, R.D. 1991. *The biology of the naked mole-rat.* Princeton: Princeton University Press.

Van Sandwyk, J.H.D.T. & Bennett, N.C. 2005. Do solitary seismic signalling Cape mole-rats (*Georychus capensis*) demonstrate spontaneous or induced ovulation? *Journal of Zoology London* 267: 75-80.

Whidden, H.P. 2000. Comparative myology of moles and the phylogeny of the Talpidae (Mammalia, Lipotyphla). *American Museum Noviatates* 1-53.

White, J. L. 1993. Indicators of locomotor habits in xenarthrans: evidence for locomotor heterogeneity among fossil sloths. *Journal of Vertebrate Paleontology*, 13: 230–242.

Wilson, L. A.B. & Geiger, M. 2015. Diversity and evolution of feroral variation in Ctenohystrica. In: Cox, P.G. & Hautier, L. *Evolution of Rodents.* Cambridge: Cambridge University Press. 510-538.